Theoretical Studies on the Structural and Spectral Properties of Silicon Sulfide Glasses

J. A. Tossell

Department of Chemistry and Biochemistry, University of Maryland, College Park, Maryland 20742

Received September 2, 1993. Revised Manuscript Received December 13, 1993®

Local structural units existing in silicon sulfide and alkali-metal silicon sulfide glasses have recently been identified by comparison of their ^{29}Si NMR spectra with those of model compounds. In constrast to silicon oxides, where the Si is shielded by corner sharing of the silicate tetrahedra and deshielded by edge sharing, the Si sulfides show only a small shielding arising from corner sharing but a substantial shielding resulting from edge sharing. To help in understanding this and other differences between the silicon oxides and sulfides, we have used ab initio quantum mechanical methods to calculate the equilibrium structures, vibrational spectra and NMR spectra for some simple molecular models of the Si sulfide species occurring in condensed phases. The compounds studied include the series SiH_4–$Si(SH)_4$, the isoelectronic compounds $SiCl_4$, SiS_4^{4-}, and $Si(SH)_4$, the tetrahedral corner-sharing molecules $(SiH_3)_2S$ and $(H_2SiS)_3$, the edge-sharing molecules $(H_2SiS)_2$, $Si_2S_4H_4$, and $Si_3S_4H_4$, the face-sharing dimer $Si_2S_3H_2$, and the edge-sharing, corner-sharing combination $Si_4S_5H_6$. Accurate structures, energetics, and vibrational spectra can be obtained for these molecules at the polarized split-valence ab initio SCF level. The calculated vibrational spectrum for $Si_3S_4H_4$ matchs well against that of solid SiS_2. However, accurate NMR shieldings require at least a doubly polarized basis on the Si and S and single polarization functions on the H. At the highest basis set level employed we find the Si in the edge-sharing dimer $(H_2SiS)_2$ to be shielded with respect to that in the corner-sharing trimer $(H_2SiS)_3$ by a few ppm, in agreement with experiment for their methylated gas-phase analogues. However, this difference between Si chemical shifts for these corner- and edge-sharing gas-phase compounds is substantially smaller than that observed in the analogous solids. We offer a qualitative explanation for this result based on the relative energies and hardnesses of edge-sharing and corner-sharing oligomers. Our calculations also reveal differences in S nuclear quadrupole coupling constants and NMR shieldings between the different species which may be useful for their characterization.

Introduction

Determination of local and midrange structure is an important problem in glass science. Many experimental techniques can be used to ascertain local structure, including X-ray diffraction, EXAFS, IR Raman, and NMR spectroscopies.[1] A particularly valuable technique for the characterization of Si-containing glasses is ^{29}Si solid-state NMR spectroscopy.[2] The success of this technique for the characterization of local order in Si oxide glasses is partly a result of the existence of numerous crystalline materials of related composition, which makes possible a "finger-printing" approach to the assignment of the spectrum of a silicate glass. It is also partly a result of the rather simple systematic dependence[3] of ^{29}Si NMR shieldings on the degree of polymerization, the angle at the bridging oxygen, and the identities of atoms in the second coordination sphere of Si.

Recently, ^{29}Si NMR has been used to study local order in Si sulfide and alkali-metal Si sulfide glasses and in related crystalline solids.[4] An important conclusion of these studies is that the Si shieldings are little affected by corner-sharing polymerization but are substantially increased by edge-sharing polymerization. This result is much different from that seen in silicates, where condensation polymerization shields the Si by about 10 ppm per corner-sharing O[3] and where smaller ring sizes are associated with smaller shieldings.[5] Our previous quantum mechanical calculations[6] also indicate that Si in the edge-sharing "2-ring" $(H_2SiO)_2$ is deshielded with respect to that in the corner-sharing "3-ring" $(H_2SiO)_3$, in contrast to the increased shielding observed in Si sulfides. Trends similar to those in the Si sulfides have also been observed for Si selenides.[7]

In a previous study, we used a decomposition over molecular orbitals of the computed Si shieldings as a function of ∠Si–O–Si in $(SiH_3)_2O$ to give a qualitative MO interpretation of the shielding trends, focusing on changes in MO energies with angle.[8] Several of the valence MOs

® Abstract published in *Advance ACS Abstracts*, January 15, 1994.

(1) Elliott, S. R. *Physics of Amorphous Materials*; Longman Press; London, 1984.

(2) Fyfe, C. A. *Solid State NMR for Chemists*; C. E. C. Press; Guelph, 1983.

(3) Kirkpatrick, R. J. MAS NMR spectroscopy of minerals and glasses. In *Spectroscopic Methods in Mineralogy and Geology*; Hawthorne, F. C., Ed.; *Rev. Mineral.* **1988**, *18*, 341.

(4) (a) Tenhover, M.; Boyer, R. D.; Henderson, R. S.; Hammond, T. E.; Shreve, G. A. *Solid State Commun.* **1988**, *65*, 1517. (b) Eckert, H.; Zhang, Z.; Kennedy, J. H. *J. Non-Cryst. Solids* **1989**, *107*, 271. (c) Eckert, H.; Kennedy, J. H.; Pradel, A.; Ribes, M. J. *Non-Cryst. Solids* **1989**, *113*, 287.

(5) Brinker, C. J.; Kirkpatrick, R. J.; Tallant, D. R.; Bunker, B. C.; Montez, B. *J. Non-Cryst. Solids* **1988**, *99*, 418.

(6) Tossell, J. A. *J. Non-Cryst. Solids* **1990**, *120*, 132.

(7) Pradel, A.; Michel-Lledos, V.; Ribes, M.; Eckert, H. *Chem. Mater.* **1993**, *5*, 377.

0897-4756/94/2806-0239$04.50/0

change both in energy and in their contribution to the NMR shielding as a function of the briding angle and the total energy as a function of angle depends upon a competition between the energetics of several different MOs. This competition may be different in Si oxides and sulfides, so it is certainly conceivable that the trend in shielding with angle in Si sulfides could be different from that in Si oxides.

In addition to their differences in Si NMR shielding trends, Si sulfides and oxides also differ substantially in the changes which occur in their IR Raman spectra as a result of polymerization and glass formation and in the relative energies of their different polymeric forms, e.g., corner- vs edge-sharing polymers. The room-temperature, atmospheric-pressure crystal structure of SiS_2 shows an edge-shared geometry, while all the well-characterized low-pressure polymorphs of SiO_2 show corner-sharing geometries. Identification of local structures in Si sulfide glasses can thus be made on the basis of energetic considerations and/or fits against experimental vibrational spectra or NMR spectra. A analysis of the of the Raman spectra[9] of crystalline and glassy SiS_2 will form an important part of this paper.

In this paper we utilize molecular quantum mechanical methods to calculate the equilibrium structures, vibrational spectra, and NMR properties for a number of molecular models for local species occurring in Si sulfide glasses. Such molecular cluster approaches have been used for some time, although they are often employed in a semiempirical way, using parameters fitted to the properties of gas-phase molecules.[10] Our goals are (1) to reproduce shielding trends caused by variations in composition and structure in the first and second coordination shells about Si, (2) to understand the electronic structural basis for such trends, (3) to establish the connection between different spectroscopic signatures for a given species, e.g., to interrelate features seen in IR Raman and NMR spectra, (4) to test the cause and effect relationships thought to underly empirical correlations of shielding and structure, (5) to assist in the identification of species existing in glasses and melts.

Several problems to be surmounted in the accurate calculation of NMR properties of condensed phase species are (1) the so-called n^4 problem—the fact that the computational resources needed for an ab initio Hartree–Fock calculation scale as about the fourth power of the size of the system or the size of the basis set used to expand the MOs, tempting us to use model systems which are too small and/or basis sets which are too small, (2) the gauge problem[11]—the dependence of results upon the choice of origin for the vector potential of the magnetic field except in the Hartree–Fock limit of an extremely large basis (although judicious choices of origin, subtraction of erroneous contributions from core electrons, and/or inclusion of particular specialized basis functions can reduce this problem), (3) the correlation problem[12]—the neglect of the instantaneous correlation of electron motions in the Hartree–Fock method leading (in general) to undershielding and exaggerated shielding anisotropies, and (4) the problem of truncating or terminating the model cluster without introducing computational artifacts. For small molecules the first three problems can essentially be overcome by employing large basis sets and fast present day computers, but for large molecules (as models for middle range order in solids will necessarily be), such constraints will seriously limit the accuracy of the results.

Our general procedure for modeling the NMR shielding in a condensed-phase species is (1) choose a particular set of model molecules, which have the same local geometries expected in the solids, (2) choose a quantum mechanical method rigorous enough to accurately reproduce the geometric structures and the vibrational spectra of these model molecules, (3) establish the stability of the calculated NMR shielding *trends* (although not necessarily the absolute values) with respect to basis set expansion, (4) test the calculated shielding trends vs those observed in related gas-phase molecules (if possible), (5) establish the stability of the calculated shielding trends vs modest enlargements of the model molecules, and (6) test the calculated shielding trends vs those assigned experimentally to particular species in the glasses.

Computational Method

The basis Hartree–Fock self-consistent-field MO theory used in this work has been thoroughly reviewed, and the errors in bond distances and vibrational frequencies expected at various computational levels for small gas-phase molecules are well understood.[13] Calculation of the equilibrium structures and vibrational spectra was done with the program GAMESS[14] while the more specialized calculation of the NMR shieldings were done mainly with the program RPAC,[15] interfaced to GAMESS, and with the program SYSMO.[16] RPAC can utilize either the conventional common-origin coupled Hartree–Fock method[17] or the random-phase-approximation localized-orbital local-origin (RPA LORG) method,[18] while SYSMO employs the common-origin CHF approach. An important advantage of the LORG method is that it treats more accurately the shielding contributions of those orbitals distant from the magnetic nucleus. The advantage of SYSMO is that it utilizes symmetry more fully and avoids the transformation of the electron repulsion integrals from AOs to MOs needed in RPAC. For some of the molecules we also present preliminary results using the gauge-including AO (GIAO) method,[19] implemented in the program TX-90.[20] Another powerful method for NMR shielding calculations is the individual gauge for local orbitals (IGLO) method.[21] LORG and IGLO methods seem to generally give quite similar results.[22] Descriptions

(8) Lindsay, C. G.; Tossell, J. A. *Phys. Chem. Miner.* **1991**, *18*, 191.
(9) Tenhover, M.; Hazle, M. A.; Grasselli, R. K. *Phys. Rev. Lett.* **1983**, *51*, 404.
(10) Lucovsky, G.; deNeufville, J. P.; Galeener, F. L. *Phys. Rev. B* **1974**, *9*, 1591.
(11) Epstein, S. T. *J. Chem. Phys.* **1973**, *58*, 1592.
(12) Bouman, T. D.; Hansen, Aa. E. *Chem. Phys. Lett.* **1990**, *175*, 292.
(13) (a) Pople, J. A. *Ber. Bunsen-Ges. Phys. Chem.* **1982**, *86*, 806. (b) Simons, J. *J. Phys. Chem.* **1991**, *95*, 1017.
(14) Schmidt, M. W.; Baldrige, K. K.; Boatz, J. A.; Jensen, J. H.; Koseki, S.; Gordon, M. S.; Nguyen, K. A.; Windus, T. L.; Elbert, S. T. *QCPE Bull.* **1990**, *10*, 52.
(15) Bouman, T. D.; Hansen, Aa. E. "RPAC Molecular Properties Package, Version 9.0"; Southern Illinois University at Edwardsville, 1991.
(16) Lazzeretti, P.; Zanasi, R. *J. Chem. Phys.* **1980**, *72*, 6768.
(17) Lipscomb, W. N. *Adv. Magn. Reson.* **1966**, *2*, 137.
(18) Hansen, Aa. E.; Bouman, T. D. *J. Chem. Phys.* **1985**, *82*, 5035.
(19) (a) Ditchfield, R. *Mol. Phys.* **1974**, *8*, 397. (b) Wolinski, K.; Hinton, J. F.; Pulay, P. *J. Am. Chem. Soc.* **1990**, *112*, 8251. (c) Hinton, J. F.; Guthrie, P. L.; Pulay, P.; Wolinski, K. *J. Magn. Reson. A* **1993**, *103*, 188.
(20) Pulay, P. "TX-90—An ab initio program system"; Department of Chemistry, University of Arkansas, 1990.
(21) Kutzelnigg, W. *Isr. J. Chem.* **1980**, *19*, 193.
(22) Facelli, J. C.; Grant, D. M.; Bouman, T. D.; Hansen, Aa. E. *J. Comput. Chem.* **1990**, *11*, 32.

Table 1. Comparison of Experimental and Calculated Structural Properties for the Edge-Sharing Solid SiS_2 and Molecules with Edge-Sharing Geometries

compd	R(Si–S), Å	∠Si–S–Si, deg	ref
	Experimental Results		
SiS_2(s)	2.133	81.2	27
$[(CH_3)_2SiS]_2$	2.152	82.5	26
	Calculated Values		
$[H_2SiS]_2$	2.150	83.3	28b
	2.145	83.5	present results
$Si_2S_4H_4$	2.124, 2.133, 2.138	84.5	
$Si_2S_6H_4$	2.133	84.3	
$Si_3S_4H_4$	2.129	84.3	
edge-shared part of $Si_4S_5H_6$	2.139, 2.130	83.8	

Table 2. Comparison of Experimental Structural Properties for the High-Pressure Corner-Sharing Polymorph of SiS_2(s), Gas-Phase $[(CH_3)_2SiS]_3$, and $(SiH_3)_2S$ and Calculated Values for $(H_2SiS)_3$, $(H_2SiS)_4$, $(SiH_3)_2S$, and the Corner-Shared Part of $Si_4S_5H_6$

	R(Si–S), Å	∠Si–S–Si, deg
Experimental Geometries		
$(SiH_3)_2S$ (gas phase, ref 29)	2.136	97.4
$[(CH_3)_2SiS]_3$ (gas phase, ref 30)	2.15 ± 0.03	110
SiS_2(s), high P, high T polymorph, ref 31	2.13	109.4
Calculated Geometries		
$(SiH_3)_2S$	2.141	108.1
$(H_2SiS)_3$	2.134	103.2
$(H_2SiS)_4$	2.127, 2.139	117.8
corner-shared part of $Si_4S_5H_6$	2.114–2.137	120.8

of the major methods and reviews of their applications can be found in the proceedings of a NATO workshop on the calculation of NMR shieldings edited by the author.[23a] The use of a core-correction[23b] to the conventional common-origin CHF method, based on the atom superposition model of Flygare and Goodisman,[23c] is also described. This simple approach corrects for inexact cancellation of diamagnetic and paramagnetic shielding contributions from core electrons not on the magnetic nucleus and has been previously applied to the Zn halides.[23d]

The standard expansion basis sets employed in our geometry and vibrational spectra calculations are the 3-21G* or 6-31G* polarized split-valence bases designed by Pople and co-workers.[24] For the most accurate of the NMR calculations on the Si sulfides doubly polarized bases were used with a 3-21G s, p basis, two 3d polarization functions on both Si and S (with exponents of 0.78 and 0.26 for Si and 1.13 and 0.38 for S) and a single 2p function with exponent of 1.10 on the H atoms.

Results

Structural Properties of Corner- and Edge-Sharing Si Sulfides. Calculated and experimental structural parameters for edge-sharing and corner-sharing geometries of Si sulfide tetrahedra are compiled in Tables 1 and 2, respectively. Pictures of the molecules considered are shown in Figure 1. For the isolated tetrahedral molecule

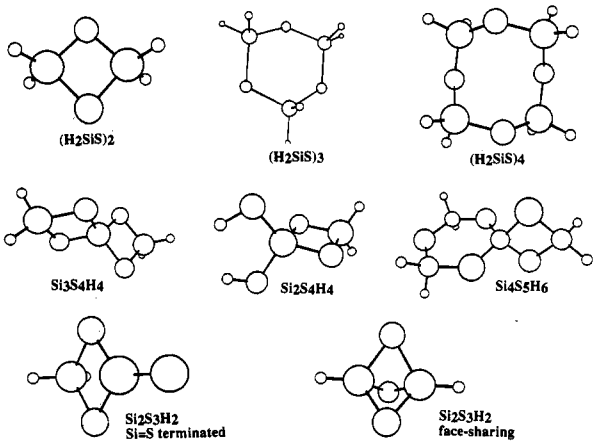

Figure 1. Calculated 3-21G* SCF equilibrium geometries for the silicon sulfide molecules $(H_2SiS)_n$, $n = 2, 3, 4$; $Si_3S_4H_4$, $Si_2S_4H_4$, $Si_4S_5H_6$ and the two isomers of $Si_2S_3H_2$. Atoms are Si, S, and H, in order of decreasing size.

$Si(SH)_4$, in S_4 symmetry, we calculate an R(Si–S) of 2.122 Å, in good agreement with the average experimental bond distance[25] in orthothiosilicates of 2.11 Å. In the edge-sharing dimer $(H_2SiS)_2$ the calculated Si–S distance is somewhat longer, in accord with experiment for the methylated analog.[26] As the size of the oligomeric unit increases, the Si–S distance is calculated to decrease slightly, for $Si_3S_4H_4$ reaching a value very similar to that observed experimentally[27] in the edge-sharing crystalline polymorph of SiS_2. The calculated ∠Si–S–Si are also in reasonable agreement with experiment, with values consistently about 2–3° too large. Our calculated structure for $(H_2SiS)_2$ is quite similar to that obtained in previous theoretical studies.[28]

For the corner-sharing species represented in Table 2 calculation and experiment are also in reasonable agreement, although our calculated ∠Si–S–Si value for $(SiH_3)_2S$ is somewhat smaller than experiment[29] and that for $(H_2SiS)_3$ somewhat smaller than that for the analog methylated gas-phase molecule.[30] The bond distances and angles observed[31] in the high-pressure corner-sharing polymorph of SiS_2 are very similar to those in $[(CH_3)_2SiS]_3$. For the "4-ring" molecule $(H_2SiS)_4$, the calculated Si–S distances are similar to those for the 3-ring but the ∠Si–S–Si is about 15° larger. No experimental information is available for "4-ring" molecules like $(H_2SiS)_4$, which have apparently never been observed. For the molecule $Si_4S_5H_6$, which has an edge-shared 2-ring connected to a corner-shared 3-ring, the calculated bond distances and angles in the corner-shared part are similar to those calculated in the smaller corner-sharing single-ring molecules, while the angles in the 3-ring part are somewhat distorted since the C_{2v} symmetry chosen for $Si_4S_5H_6$ constrained the 3-ring to be planar.

Energetics of Silicon Sulfide Rings. Our calculations give energies per H_2SiS unit of −684.3093, −684.3671,

(23) (a) Tossell, J. A., Ed. *Nuclear Magnetic Shieldings and Molecular Structure*; Kluwer: Dordrecht, 1993. (b) Tossell, J. A. In ref 23, pp 279–296. (c) Flygare, W. H.; Goodisman, J. *J. Chem. Phys.* **1968**, *49*, 3122. Tossell, J. A. *Chem. Phys. Lett.* **1990**, *169*, 145.

(24) Hehre, W. A.; Radom, L.; Schleyer, P. v. R.; Pople, J. A. *Ab Initio Molecular Orbital Theory*; Wiley: New York, 1986.

(25) Geisinger, K. L.; Gibbs, G. V. *Phys. Chem. Miner.* **1981**, *7*, 204.

(26) Schklower, W. E.; Strutschkov, Y. T.; Guselnikow, Wolkowa, W. W.; Awakyan, W. G. *Z. Anorg. Allg. Chem.* **1983**, *501*, 153.

(27) Peters, J.; Krebs, B. *Acta Crystallogr. B* **1982**, *38*, 1270.

(28) (a) O'Keeffe, M.; Gibbs, G. V. *J. Phys. Chem.* **1985**, *89*, 4574. (b) Kudo, T.; Nagase, S. *J. Am. Chem. Soc.* **1985**, *107*, 2589.

(29) Almenningen, A.; Hedberg, K.; Seip, R. *Acta Chem. Scand.* **1963**, *17*, 2264.

(30) Yokoi, M.; Nomura, T.; Yamasake, K. *J. Am. Chem. Soc.* **1955**, *77*, 4484.

(31) Prewitt, C. T.; Young, H. S. *Science* **1965**, *149*, 535.

−684.3747, and −684.3724 hartree atomic units for $(H_2SiS)_n$ with $n = 1, 2, 3$, and 4, respectively (1 hartree atomic unit per molecule equals 2625.5 kJ/mol). The 3-ring is thus calculated to be more stable than the 2-ring by about 20 kJ/mol (of H_2SiS) and more stable than the 4-ring by 6 kJ/mol. The experimentally observed 2-ring oligomer is estimated[32] to be 12 kJ/mol less stable than the 3-ring oligomer for molecules of the type $[(CH_3)_2SiS]_n$. It thus seems that thermodynamics alone would not preclude the existence of 4-ring compounds, although such species have not been observed. For molecules of type $[(SH)_2SiS]_n$, $n = 2$ and 3, (where −H has been replaced by −SH) we have carried out symmetry-restricted geometry optimizations and comparing D_{2h} and D_{3h} symmetry optimized energies for the 2- and 3-rings (not the lower energy but computationally more demanding C_{3v} 3-ring structure) we find that the two-ring is stabilized with respect to the 3-ring by about 30 kJ/mol when −H is replaced by −SH. Therefore, when the first coordination shell of the Si consists *entirely* of S, the edge-shared 2-ring structure is calculated to be more stable than the corner-shared 3-ring. This may explain why gas-phase molecules of the type $(R_2SiS)_n$ adopt 3-ring structures while 2-rings are more stable in crystalline SiS_2. For the analogous Si oxides we find the 3-ring to be more stable than the 2-ring by 72 kJ/mol of H_2SiO. In agreement with previous investigators[28a] we can thus conclude that the relative stability of the 2-ring compared to the 3-ring is significantly higher in the Si sulfides than in the oxides, or equivalently that the ring strain in the 2-ring is less in the sulfide than in the oxide.

Recently, there has been a serious attempt to quantitatively define a quantity known as the "hardness" and to develop a "principle of maximum hardness" to establish the relative stabilities of different structures for both molecules and solids.[33,34] Although the hardness is defined in density functional theory as a second derivative of the energy with respect to the number of electrons, it is expected to scale with the size of the HOMO–LUMO gap. For $(H_2SiS)_n$, we calculate HOMO–LUMO eigenvalue differences of 12.65 eV for $n = 2$, 12.59 eV for $n = 3$, D_{3h} symmetry and 13.17 eV for $n = 3$, C_{3v} symmetry. These are consistent with the calculated relative stabilities of these molecules, with the most stable molecule, $(H_2SiS)_3$, in C_{3v} symmetry having the greatest HOMO–LUMO gap and therefore the greatest hardness. For $[(SH)_2SiS]_n$, we find a HOMO–LUMO gap of 12.36 eV for $n = 2$ and 12.17 eV for $n = 3$, D_{3h}, consistent with the greater calculated stability of the $n = 2$ oligomer. Inspection of orbital eigenvalues indicates that most of the change in the HOMO–LUMO gap comes from changes in the LUMO energy.

Vibrational Spectra of Silicon Sulfides and Related Molecules. Calculated vibrational energies for the $SiCl_4$ and $(SiH_3)_2S$ gas-phase molecules are shown in Table 3. Hartree–Fock SCF calculations with polarized split valence basis sets typically overestimate vibrational frequencies[24] by about 10%, so we tabulate as well the calculated frequencies multiplied by 0.9. These scaled vibrational frequencies are in reasonably good agreement with experiment.[35,36] To exactly match the experimental energy of the a_1 totally symmetric stretching vibration of $SiCl_4$, we would need to multiply the calculated value by 0.934, as is shown in Table 3. We therefore choose this 0.934 scaling factor (rather than 0.9) for estimating the vibrational spectra of the larger Si sulfide molecules as well, since we are particularly interested in obtaining accurate energies for symmetric stretching vibrations, which are the most securely assigned features in the spectra of the solids.

Table 3. Calculated Vibrational Spectral Energies (in cm^{-1}) for $(SiH_3)_2S$ and $SiCl_4$, Scaled and Compared with Experiment

	type of vibration		
	sym bend	sym stretch	asym stretch
$(SiH_3)_2S$, calc	181	493	562
calc scaled by 0.9	163	444	506
calc scaled by 0.934	169	460	525
$(SiH_3)_2S$, exp, ref 36	159	480	508

	symmetry of vibration			
	e	t_2	a_1	t_2
$SiCl_4$, calc	165	243	454	670
calc scaled by 0.9	148	219	409	603
calc scaled by 0.934 to exactly fit exp a_1 vibration	154	227	424	626
$SiCl_4$, exp, ref 35	150	221	424	610

Assigning the spectra of solid SiS_2 based on the calculated spectra for Si sulfide molecules is a good deal more difficult than making assignments for the gas-phase molecules. According to the assignments given in the experimental study,[9] the features at 138, 175 and 181, 430, and 625 cm^{-1} in the spectrum of crystalline SiS_2 and at 121, 174, 427, and 625 cm^{-1} in the spectrum of the glass should correspond to the e, t_2, a_1, and t_2 symmetry vibrations within the SiS_4 unit. Of these only the a_1 peak, at 430 cm^{-1} in the crystal or 427 cm^{-1} in the glass, is polarized, as would be expected for a totally symmetric a_1 vibration.[37] A feature at 351 and 367, 381 cm^{-1} in the spectra of the crystal and glass, respectively, reported in ref 9 to also be polarized, has been identified as a second a_1 symmetry peak (it has been designated a_1^B, a "companion" of the SiS_4 a_1 peak) and has been assigned to a symmetric stretching motion of the S atoms of the shared edges.[9] For $SiSe_2$ an analog peak has been given a different assignment, attributing it to a b_{1g} symmetry vibration.[38]

For $Si(SH)_4$, with S_4 symmetry and nine atoms, the spectrum is of course a bit more complicated than that for a five-atom T_d symmetry molecule like $SiCl_4$. Eight of the vibrations of $Si(SH)_4$ involving mainly motion of the H atoms have frequencies above 800 cm^{-1}, but there are also two torsional modes below 100 cm^{-1} with substantial H character and a doubly degenerate mode at 304 cm^{-1} which has considerable H character. The Si–S analogs of the e, t_2, a_1, and t_2 vibrations of $SiCl_4$ (with both the e and the t_2 now split by the lowered symmetry) can be identified at scaled energies of 142 and 182 (split e), 191 and 215 (split t_2), 381 (a_1), and 549 and 566 (split t_2) cm^{-1}, as indicated in Table 4. These calculated values for $Si(SH)_4$

(32) Moedritzer, K. *J. Organomet. Chem.* **1970**, *21*, 315.
(33) Pearson, R. G. *Acc. Chem. Res.* **1993**, *26*, 250.
(34) Galvan, M.; Dal Pino, A., Jr.; Joannopoulos, J. D. *Phys. Rev. Lett.* **1993**, *70*, 21.
(35) Nakamoto, K. *Infrared Spectra of Inorganic and Coordination Compounds*, 4th ed.; Wiley: New York, 1986.
(36) Ebsworth, E. A. V.; Taylor, R.; Woodward, L. A. *Trans. Faraday Soc.* **1959**, *55*, 211.
(37) Ebsworth, E. A. V.; Rankin, D. W. H.; Cradock, S. *Structural Methods in Inorganic Chemistry*; Blackwell: Oxford, 1987.
(38) Griffiths, J. E.; Malyj, M.; Espinosa, G. P.; Remeika, J. P. *Phys. Rev. B* **1984**, *30*, 6978.

Table 4. Calculated Vibrational Spectral Energies (in cm^{-1}) for $Si(SH)_4$, $(H_2SiS)_n$, n = 2 and 3, $Si_3S_4H_4$, $Si_2S_4H_4$, and $Si_4S_5H_6$, Scaled and Compared with Experimental Data[9] for Solid Forms of SiS_2

$Si(SH)_4$, calc (Si–S modes)	152, 195 (split e)	205, 230 (split t_2)	408 (a_1)	588, 606 (split t_2)
calc scaled by 0.934	142, 182	191, 215	381	549, 566
$(H_2SiS)_2$ D_{2h} symmetry			335 (a_g) S sym breathing	
calc scaled by 0.934			313	
$(H_2SiS)_3$			287 (a_1)	
C_{3v} symmetry			S sym breathing	
calc scaled by 0.934			268	
$Si_3S_4H_4$		208 (e)	370 (b)	591 (e)
S_4 sym		217 (a)	450 (a)	643 (b)
			484 (e)	648 (e)
			535 (b)	
			545 (a)	
calc scaled by 0.934		194	346	561
		203	420	601
			452	605
			500	
			509	
$Si_2S_4H_4$			310 (a_1)	484 (b_1)
C_{2v} sym			435 (a_1)	543 (a_1)
calc, scaled by 0.934			290	452
			406	507
$Si_4S_5H_6$		204 (b_1)	346 (a_1)	486 (b_1)
C_{2v}		274 (a_1)	3-ring breathing	502
			397 (a_1) 2-ring, 3-ring breathing	
			466 (a_1) SiS_4 sym stretch	
calc, scaled by 0.934		190	323	454
		256	371	469
			435	
exp SiS_2, $Si(S_{1/2})_4$ modes[9]				
crystal	138 (e)	175, 181	430 (a_1)	625 (t_2)
glass	121	174	427	625
$Si_2(S_{1/2})_8$ modes[9]				
crystal			351 (a_1^B)	
glass			367, 381 (a_1^B)	
additional features in spectrum			340	585
of glass			370	

show a similar pattern to the experimental values for SiS_4-like vibrations in solid SiS_2 but do not match very well against them quantitatively.

A much better fit to the experimental spectrum of solid SiS_2 is obtained from our calculation on $Si_3S_4H_4$, where the central Si has the correct number and type of neighbours in both its first and second coordination shells. In this S_4 symmetry molecule the normal modes are of a, b, and e type. All the modes are Raman active with the a mode polarized, and all the modes except a are also IR active. Although we do not presently have the capability of calculating Raman intensities, we generally would expect the totally symmetric a_1-like vibrations to have the largest Raman intensity.[37] Vibrations with scaled calculated energies of 420 and 346 cm^{-1} as shown in Table 4 are identified with the a_1 and the so-called a_1^B features seen in the experimental spectrum. The calculated normal modes corresponding to these frequencies are shown in Figure 2. While the mode at 420 cm^{-1} is indeed a simple symmetric stretching mode of the S atoms connected to the central Si, expected on the basis of the qualitative analysis, the feature at 346 cm^{-1} is *not* a simple symmetric stretch of the S atoms of the shared edge as often suggested by qualitative pictures. In fact, the corresponding mode in $Si_3S_4H_4$ is of b symmetry, consistent with its assignment by Griffiths et al. to a b_{1g} symmetry mode in the crystal.[38] This mode is basically a ring-breathing mode in which one pair of S atoms moves toward the chain axis and the next pair moves away from the axis, but it also contains contributions from antisymmetric motions of the Si atoms. It is much less localized spatially than the totally symmetric a mode at 420 cm^{-1}. We would thus expect the b symmetry mode to be more sensitive to medium and long-range order within the material and thus to show a range of energies in a glass. The calculated spectrum for $Si_3S_4H_4$ also shows an additional feature, calculated at a scaled value of 452 cm^{-1}, which transforms as e, and so is both IR and Raman active. There is a shoulder in the Raman spectrum of crystalline SiS_2 at about 450 cm^{-1}, which could correspond to this vibration.

In Figure 3 we superimpose on the experimental Raman spectrum of crystalline SiS_2 from ref 9 our scaled calculated values of 194, 203, 346, 420, 452, 509, and 606 cm^{-1} for $Si_3S_4H_4$. These constitute all the calculated vibrations in the range 150–650 cm^{-1} which have a calculated IR intensity less than 1.0 $D^2/(amu \times Å^2)$. We anticipate that these vibrations with low IR intensity will generally have large Raman intensity. The only calculated feature inconsistent with the experimental spectrum is the normal-mode vibration at 509 cm^{-1}, which corresponds to a breathing mode of the exterior $-SiH_2$ groups of the $Si_3S_4H_4$ molecule and thus may be considered an artifact of the cluster model. Agreement of the other scaled calculated vibrational energies of $Si_3S_4H_4$ with experiment is quite good.

In the simpler 2-ring $[H_2SiS]_2$ a symmetric ring breathing mode of the S atoms is calculated to occur at a scaled value of 313 cm^{-1}. In the equilibrium C_{3v} geometry of $[H_2SiS]_3$ there is a S symmetric breathing mode calculated at a scaled value of 268 cm^{-1}. These modes are also shown in Figure 2. However, the S breathing modes in $(H_2SiS)_n$ all involve significant $-SiH_2$ motion as well. By analogy

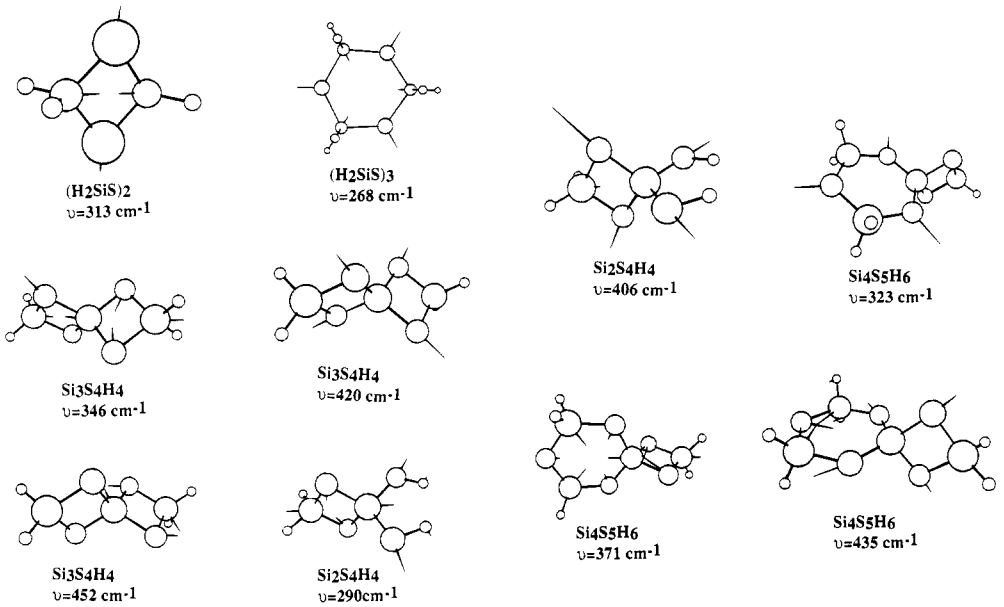

Figure 2. Some of the calculated vibrational normal modes of $(H_2SiS)_n$, n = 2, 3, $Si_3S_4H_4$, $Si_2S_4H_4$, and $Si_4S_5H_6$, with scaled calculated energies as indicated. The arrows indicate the directions and relative magnitudes of the nuclear displacements.

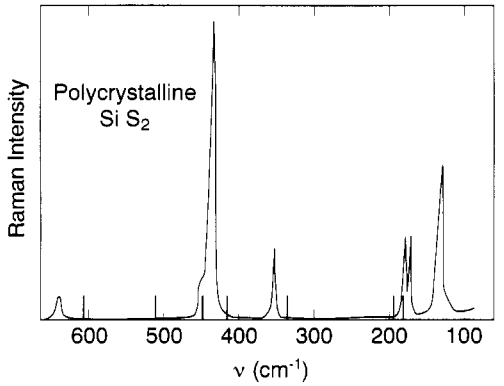

Figure 3. Experimental Raman spectrum of crystalline SiS_2 (from ref 9) with calculated scaled frequencies of 194, 203, 346, 420, 452, 509, and 605 cm^{-1} from/$Si_3S_4H_4$ superimposed as vertical lines.

with the $(H_2SiO)_n$ rings previously studied,[6] we would certainly expect the breathing frequencies to decrease with increasing ring size, as calculated. However, for the oxides, the symmetric breathing motion of the anions is almost "pure", i.e., the motion of the $-SiH_2$ groups is very slight in these normal modes, and the Raman features arising from them in Si oxides are quite narrow.[39] In the sulfides the rings are considerably more puckered and the symmetric breathing modes less pure. The Raman spectral features of such rings within the solid would thus be broad, not sharp as in the Si oxides.

The simplest possible model for the breaking of the edge-shared Si sulfide chain would be $Si_2S_4H_4$, with a terminal $-SiH_2$ group removed from $Si_3S_4H_4$ and the dangling bonds on the S atoms protonated (see Figure 1). The scaled a_1 vibrational energy for this molecule is lower by about 14 cm^{-1} than that in $Si_3S_4H_4$ while the analog of the b symmetry vibration is lowered by 56 cm^{-1}. The simplest molecule we can study which incorporates both edge-shared and corner-shared SiS_4 groups, as in the cross-linked chain cluster, or CLCC, model of Griffiths et al.,[38] is the $Si_4S_5H_6$ molecule, also shown in Figure 1, which is essentially an edge-shared 2-ring connected to a corner-shared 3-ring. This molecule shows scaled vibrational energies of 323, 371, and 435 cm^{-1}, whose calculated normal modes are shown in Figure 2. The mode at 323 cm^{-1} is basically a symmetric breathing mode of the S atoms of the 3-ring, that at 371 cm^{-1} an analog of the b vibration of $Si_3S_4H_4$, and that at 435 cm^{-1} is an a_1 symmetric stretching mode of the S atoms about the central Si.

The experimental spectrum of glassy SiS_2 shows, compared to that of the crystalline solid, an apparent broadening of the "a_1^B" absorption around 350 cm^{-1} and two additional features in the region 360–380 cm^{-1}. We associate these with a_1^B-type vibrations in species in which the edge-sharing chain is broken (the $Si_2S_4H_4$ model) or is mixed with a corner-sharing chain (the $Si_4S_5H_6$ model). The amorphous material also shows broadening in the region of the main a_1 peak, which appears to have shoulders on both its low- and high-energy sides, again consistent with contributions from $Si_2S_4H_4$- and $Si_4S_5H_6$-like species. The existence of discrete 3-rings is probably excluded by the absence of absorption around 287 cm^{-1}, where the symmetric stretch of $(H_2SiS)_3$ is calculated to occur, although this feature might be broadened so much as to be difficult to identify.

Effects of Corner and Edge Sharing on the ^{29}Si NMR Shieldings of Oxides. Before considering the effect of polymerization on the ^{29}Si NMR parameters of Si sulfides, it is worthwhile to review related effects for the Si oxides. In interpreting the experimental chemical shifts and calculated NMR shielding constants reported in Tables 5–9, it is important to keep in mind the IUPAC shift convention for Si, which is that more positive chemical shifts, δ, correspond to less positive values of the shielding constant, σ. As shown in Table 5, the experimental data[40] show that oligomerization, involving corner sharing of O, leads to an increased shielding of the Si (i.e., a less positive δ) in compounds of the type $(CH_3)_nSi(OCH_3)_{4-n}$. Similar results are observed in other siloxanes[41] as well as in

(39) Galeener, F. L. *J. Non-Cryst. Solids* **1982**, *49*, 53.

(40) Marsmann, H. ^{29}Si NMR spectroscopic results. In *^{17}O and ^{29}Si NMR: NMR Basic Principles and Progress*; Diehl, P., Fluck, E., Kosfeld, R. Eds.; Springer: Berlin, 1981; Vol. 17.

(41) Bertling, E.; Marsmann, H. C. *Phys. Chem. Miner.* **1988**, *16*, 295.

Table 5. Experimental and Calculated Effects of Sharing Corners in Si Oxides

	One Corner Shared		
experimental (from ref 40)			
	monomer	dimer	
	$(CH_3)_3SiOCH_3$	$(CH_3)_3SiOSi(CH_3)_3$	
δ_{exp}	+17.0–17.75	6.0–7.2	
calculated			
	SiH_3OH	$H_3SiOSiH_3$	
		∠Si—O—Si= 140	180
σ_{calc} LORG,6-31G**	446	455	472
	Two Corners Shared		
experimental			
	monomer	dimer	trimer
	$(CH_3)_2Si(OCH_3)_2$	$[(CH_3)_2SiO]_n$	
		$n = 2$	$n = 3$
δ_{exp}	−2.5	na	−8.9 to −9.9
calculated			
	$SiH_2(OH)_2$	$[H_2SiO]_n$	
		$n = 2$	$n = 3$
σ_{calc}	442	424	459

Table 6. Experimental NMR Shifts in Siloxane Monomer and Ring Oligomers

	δ_{exp} (ref 40)
$(CH_3)_2Si(OCH_3)_2$	−2.5
$[RR'SiO]_2$, R, R′ = mes, xyl	−3.0 to −3.6[a]
$[(CH_3)_2SiO]_3$	−8.9 to −9.9
$[(CH_3)_2SiO]_4$	−19.5 to −20.2
$[(CH_3)_2SiO]_5$	−21.7 to −22.8
$[(CH_3)_2SiO]_6$	−22.5 to −23.0

[a] Reference 42.

Table 7. Calculated Trend in Si NMR Shielding for the Series $SiH_{4-n}(SH)_n$ vs the Experimental Trend for $SiH_{4-n}(SCF_3)_n$ (Ref 44)[a]

	n							
	0		1		2		3	
σ^{Si}_{calc}	528		494		465		440	
$\Delta\sigma_{calc}$		34		29		25		
δ_{exp}	−93		−53		−23		1	
$-\Delta\delta_{exp}$		40		30		24		

[a] Calculations employ 3-21G* optimized geometries, a doubly polarized 3-21G basis and the LORG method.

Table 8. Experimental[40] and Calculated Effects of Sharing One Corner in Si Sulfides

	$(CH_3)_3Si(SCH_3)$	$(CH_3)_3SiSSi(CH_3)_3$		
δ_{exp}	+16.6	+12.8		
	$SiH_3(SH)$	$(SiH_3)_2S$		
		∠Si—S—Si= 90	108	120
σ_{calc}[a]	494	466	484	488

[a] LORG calculation with 3-21G plus double 3d Si, S, H2p basis.

silicates.[3] As is also shown in the Table 5, calculations on related compounds with –H replacing $-CH_3$ using the LORG method with polarized split valence 6-31G** bases[24] show that increased shielding (i.e., a more positive σ) results from sharing an O corner. The effect of sharing two corners is observed experimentally and theoretically to be about twice as large as that of sharing only one.

The data in Table 6 also indicate that the shielding depends substantially on ring size, with edge-sharing 2-ring compounds deshielded compared to corner-sharing 3-ring compounds and the 3-ring compounds slightly deshielding with respect to 4- and larger rings.[40] This comparison is not completely clear cut, however, since the 2-ring compounds are unstable unless the groups terminating the Si are large, such as the hydrocarbon groups mes or xyl. Nonetheless, all 2-rings so far synthesized show a deshielding of the Si compared to the results for larger rings.[4] Previous studies[6] using common-origin coupled Hartree–Fock techniques indicated an increased shielding with increase of ring size. Although these results are qualitatively correct, the shielding trend may be exaggerated by our failure in that study to correct for distant core effects. When distant core corrections are added, the trends are the same but the magnitude of the calculated shielding difference between 2-ring and 3-rings is reduced. Using the LORG method, 6-31G** basis sets and 3-21G* optimized geometries we calculate Si NMR shieldings of 424 and 459 ppm for the $(H_2SiO)_n$, $n = 2, 3$ rings, respectively. The calculated shielding difference of 35 ppm is smaller than the previous common-origin CHF value of 54 ppm[6] but is still substantial.

Table 9. Calculated Values of the Si NMR Shielding in the $SiH_2(SH)_2$ Monomer and in Small Oligomeric Rings Compared with Experimental[47] Chemical Shift Values

		oligomers	
	monomer $SiH_2(SH)_2$	$[H_2SiS]_2$	$[H_2SiS]_3$
	σ_{calc}		
LORG			
3-21G*	481	477	481
3-21G+ DSi3d, DS3d, H2p	465	460	
CHF, core-corrected			
3-21G+ DSi3d, DS3d, H2p	451	437	434 (447[a])
GIAO			
6-31G**		452	453
6-31G + DSi3d, DS3d, DH2p		453	452

	$(CH_3)_2Si(SCH_3)_2$	$[(CH_3)_2SiS]_2$	$[(CH)_2SiS]_3$
δ_{exp}	28.1	16.6	20.9

[a] D_{3h} optimized 3-21G* geometry used instead of C_{3v} optimized geometry.

Previous common-origin CHF studies[43] indicated that decreasing the Si–O–Si angle in $(SiH_3)_2O$ decreased the Si shielding, in agreement with experiment. The present LORG results with 6-31G* bases also show the Si shieldings in $(SiH_3)_2O$ to decrease as the ∠Si–O–Si decreases, with a difference of about 17 ppm between bridging angle values of 140 and 180°. Thus, although the LORG method used in this work is different in some important respects from the common-origin coupled Hartree–Fock method applied previously to Si oxides, the calculated trends as a function of degree of polymerization and bridging angle are the same—Si in oxides is calculated to be shielded by corner-sharing polymerization and deshielded by edge-sharing polymerization and the shielding decreases as the ∠Si–O–Si angle decreases.

The variation of the ^{29}Si NMR shielding in the $(CH_3)_nSi(OCH_3)_{4-n}$ series has recently been calculated using the GIAO method.[19c] The least shielded compound, with a chemical shift $\delta = +17$ (Table 5), was that for $n = 3$ and calculation and experiment were in good agreement (note that the relative shielding scale used in Table 1 of ref 19c is the negative of the chemical shift scale used in Table 5).

Shielding Changes along the $SiH_{4-n}(SH)_n$ Series. Since an examination of the effects of corner- and edge-

(42) Yokelson, H. B.; Millevolte, A. J.; Adams, B. R.; West, R. *J. Am. Chem. Soc.* **1987**, *109*, 4116.

(43) Tossell, J. A.; Lazzeretti, P. *Phys. Chem. Miner.* **1988**, *15*, 564.

sharing of shielding can be most economically performed if we use compounds with some terminating H atoms rather than all -SH groups, e.g., $SiH_3(SH)$ as the monomeric unit, it is important to establish that we can correctly reproduce the shielding trend along the $SiH_{4-n}(SH)_n$ series. In Table 7 we show calculated values of the Si NMR shielding for this series compared with experimental values[44] for the series $SiH_{4-n}(SCF_3)_n$. The calculated trend is in the right direction and of the right magnitude and the differences from one compound to another are reproduced rather well (compare the $\Delta\sigma_{calc}$ and $-\Delta\delta_{exp}$ rows). These calculations employed 3-21G* optimized geometries and a 3-21G basis set with two 3d polarization functions on both Si and S and single 2p polarization functions on the H. The standard 3-21G* basis gave the right trend in shieldings, but the calculated differences from one compound to the next were about a third smaller than those calculated with the larger basis.

Shieldings of SiS_4^{4-} and $Si(SH)_4$ Compared to That of $SiCl_4$. We also need to establish that we can correctly describe the shieldings of unpolymerized Si sulfides compared to various standards, e.g., compared to the isoelectronic gas-phase molecule $SiCl_4$, with which the Si sulfides are often compared. The SiS_4^{4-}, $Si(SH)_4$, and $SiCl_4$ molecules all show a substantial basis set dependence in their calculated shieldings and a modest difference btween LORG and core-corrected CHF shieldings. Our best calculation for $SiCl_4$ used the core-corrected CHF method with triple-ζ s, p bases and two d-polarization functions on both Si and Cl and gave a shielding of 378 ppm, in reasonably good agreement with the experimental value[45] of 400 ppm. At this large basis set level the SiS_4^{4-} molecule is slightly deshielded and $Si(SH)_4$ is strongly deshielded (shieldings of 371 and 349 ppm, respectively) with respect to $SiCl_4$. Smaller basis sets, such as the 3-21G*, actually give the sulfides as more shielded than $SiCl_4$, using either the core-corrected CHF or LORG methods. In previous studies on Si oxides[46] we found the free SiO_4^{4-} anion to be shielded by about 15 ppm compared to geometry-optimized S_4 symmetry $Si(OH)_4$. The analog Si sulfide species show a similar difference. Assuming that the neutral species provides a better representation for the SiS_4 unit within a condensed phase, we calculate thiosilicates with unpolymerized structures to be deshielded by about 29 ppm vs $SiCl_4$ (which has $\delta_{exp} = -18$, ref 40), leading to a shift of about $\delta = +11$ ppm, in about the range observed[4b] for orthothiosilicates, like Na_4SiS_4.

Changes in Si Shielding Produced by Corner-Sharing in Si Sulfide dimers. We can now begin to explore the effect of the sharing of polyhedral element (corners, edges, and faces) on the Si shielding in Si sulfides. Experimental and calculated effects of corner sharing on the shieldings are illustrated in Table 8. The first point to note is that for the $(CH_3)_3Si(SCH_3)$ monomer dimerization by corner-sharing is found experimentally[40] to shield the Si by only about 4 ppm, considerably less than the approximate 10 ppm effect seen in the analog oxides (compare Table 5). We also see that for $(SiH_3)_2S$ decreasing the $\angle$Si-S-Si decreases the calculated shielding, the *same* shielding vs bridging angle trend observed for oxides. Due to the steep dependence of total energy on angle for the Si sulfides[25] we have considered only two arbitrary angles of 90° and 120°, in addition to the calculated equilibrium angle of 108°. Nonetheless, the change in shielding within this small angular range is substantial.

Although the calculated shieldings of the H-terminated monomer and dimer do not reproduce the experimental trend for the methylated compounds, they do confirm that corner-sharing produces a smaller increase in shielding in the sulfides than in the oxides. The discrepancy between calculation and experiment is probably related to the difference in the shielding due to a -SH group, used in the calculations, and that due to the $-SCH_3$ group used in the experimental comparison. On the basis of experimental chemical shifts of $\delta = +39$ for $Si(SCH_3)_4$, +11 for $Si(SCF_3)_4$, and about +10 for SiS_4 in orthothiosilicates, we expect that replacement of a single -SH group by a $-SCH_3$ group should deshield the Si by about 7 ppm. We have in fact calculated the shielding of $SiH_3(SCH_3)$ using the same type of basis as for $SiH_3(SH)$ and we obtain a value of 490 ppm, 4 ppm smaller than in $SiH_3(SH)$. Even with this correction, however, we still calculate the dimer to be slightly deshielded with respect to the monomer. The measurable difference of -SH and $-SCH_3$ group effects is in contrast to the very similar effects of -OH and $-OCH_3$ groups on Si NMR shieldings. For example, the NMR shift of $Si(OCH_3)_4$ is -79 ppm, only a few ppm more shielded than is typical for nesosilicates.[40]

Changes in Si Shielding Produced by Edge-Sharing or Corner-Sharing in Silicon Sulfide Oligomeric Rings. In Table 9 we consider the change in shielding produced by condensation polymerization of the $SiH_2(SH)_2$ monomer to form an edge-shared 2-ring or a corner-shared 3-ring. Experimentally, for the analog gas-phase methylated compounds, the 3-ring is shielded with respect to the monomer by about 7 ppm and the 2-ring is shielded by about 12 ppm.[47] These trends are in the same direction as those seen experimentally in solid Si sulfides,[4b] where the two-corner-shared (or Q^2) species are generally shielded by about 5 ppm with respect to the unpolymerized species (Q^0) and the one-edge-shared (or E^1) species is shielded by about 15 ppm compared to Q^0. Estimating the shielding of $SiH_2(SCH_3)_2$ to be about 451 ppm at the LORG, 3-21G + DSi3d, DS3d, H2p level (14 ppm smaller than the calculated value for $SiH_2(SH)_2$), we find that the compound $(H_2SiS)_2$ is calculated to be shielded by about 9 ppm compared to the methylated monomer. We are not presently able to calculate the shielding of $(H_2SiS)_3$ using LORG at the doubly polarized basis set level due to integral storage limitations and so cannot obtain a similarly accurate value for the LORG shielding of the 3-ring. When a 3-21G* basis is used for both 2- and 3-rings the shielding of the 2-ring compound is 477 ppm and that of the 3-ring is 481 ppm, the *opposite* of the experimental ordering. Common-origin CHF calculations with larger basis sets and standard core corrections give a slightly smaller shielding for the 3-ring than for the 2-ring, but since the core correction is an approximation this result is not definitive. If the symmetry of the three-ring is constrained to D_{3h}, it has a higher Si shielding than the two-ring, even when the core-corrected CHF method is used. Further preliminary calculations[48] using the GIAO method are also reported in Table 9, confirming the core-corrected CHF results. Using a 6-31G** basis set and optimized geom-

(44) Haas, A.; Vongehr, M. *Z. Anorg. Allg. Chem.* **1978**, *447*, 119.
(45) Jameson, C. J.; Jameson, A. K. *Chem. Phys. Lett.* **1988**, *149*, 300.
(46) Tossell, J. A. *Phys. Chem. Miner.* **1991**, *17*, 654.
(47) Wojnowski, W.; Pikies, J. *Z. Anorg. Allg. Chem.* **1984**, *508*, 201.
(48) Saghi-Szabo, G., Tossell, J. A., manuscript in preparation.

etries, the GIAO calculations show the 3-ring to be very slightly more shielded than the 2-ring, but when a doubly polarized basis is used to calculate both the geometries and the shieldings, this difference is reversed and the 3-ring becomes slightly (2 ppm) less shielded.

What is very clear from the calculations is the difference between the Si oxides and sulfides. For the oxides, the 2-ring is clearly deshielded with respect to the 3-ring while for the Si sulfides the 2-ring and 3-ring have very similar shieldings, so that calculations with slightly different methods and/or basis sets can give different orderings.

We have also obtained preliminary results for the shieldings of $Si_3S_4H_4$ and $Si_2S_4H_4$, using the LORG method with a 3-21G* basis on the Si atom bonded to the four sulfurs and a STO-3G basis on all the other atoms. For $Si_3S_4H_4$ we obtain a shielding of 423 ppm and for $Si_2S_4H_4$ we obtain 428 ppm. Therefore, at this level of theory, breaking the edge-sharing chain increases the shielding. By comparison the same method applied to $Si(SH)_4$ gives a Si shielding of 431 ppm so that at this singly polarized basis set level we calculate edge-sharing to deshield the Si. To obtain the experimentally observed trend of increased shielding with edge-sharing, we probably need to go to a higher basis set level.

Changes in Vibrational Spectra and Si NMR Shielding Produced by Face-Sharing Geometries and Terminal Si=S Bonds. Although most discussions of the structure of amorphous SiS_2 have focused on corner- or edge-shared oligomers of tetrahedrally coordinated Si, a model considered (but then rejected) by Griffiths et al.[38] for glassy $SiSe_2$ involved extended chains terminated by Si=Se(S) double bonds (their Figure 4b). Such a model is easily amenable to theoretical study. For completeness, face-sharing geometries of tetrahedrally coordinated Si should also be considered. There are two isomeric molecules with empirical formulas $Si_2S_3H_2$ which can serve as models for such species, both of which are shown in Figure 1. One of these compounds contains a Si which is coordinated to two S atoms across a shared edge to Si and is linked to a third S atom by a double bond. Our calculated Si–S bond distances for this compound at the 3-21G* SCF level are 2.099 (across the shared edge) and 1.917 Å (to the terminal S atom). The energy change calculated at the 3-21G* SCF level for addition of this molecule to a H_2SiS monomer to give the $Si_3S_4H_4$ molecule is $\Delta E = -97$ kJ/mol of $Si_3S_4H_4$ formed, indicating that such a Si=Si terminated compound would be highly unstable. The face-sharing isomer of $Si_2S_3H_2$ is even higher in energy (by 76 kJ/mol), so it is also not expected to be an important component in the structure of the solid. A terminating Si—S group also has a distinctive spectral signature, with a Si=S stretch calculated to occur at a scaled energy of about 800 cm^{-1} and a Si NMR signal deshielded by about 135 ppm compared to $Si(SH)_4$. Since such extreme spectral signatures are apparently not seen in either the Raman or the NMR spectra of Si sulfide glasses, there is no experimental evidence to support the existence of such a species.

Other Properties Potentially Diagnostic of Local Geometry in Si Sulfides: Ionization Potentials, X-ray Absorption Term Energies and Electric Field Gradients at S. Although sulfide glasses have been studied mainly using IR Raman and NMR spectroscopy, there are other tools of potential utility for the elucidation of local and midrange structure. While X-ray or neutron diffraction and EXAFS can yield structural information directly, indirect information on geometric structure can also be obtained from photoelectron spectroscopy, X-ray absorption near-edge spectroscopy and from NMR of the quadrupolar nucleus ^{33}S, characterized by both its nuclear quadrupolar coupling constant and its NMR shielding. As shown in Table 10, although the ionization potential of the HOMO (evaluated at the Koopmans' theorem level as the negative of the orbital eigenvalue) changes imperceptibly, the Si 1s core IP increases slightly from the –SH-terminated chain to the 3-ring-terminated chain to the edge-shared chain. The XANES term energy of the LUMO can be approximated using the equivalent ionic core virtual orbital model,[49] in which the core excited atom is replaced by one with atomic number increased by 1. For example, core excited Si is represented by P, and the entire molecule is given a posigive charge. This procedure has recently been proven successful for compounds of S.[50] The term energy (energy below the ionization threshold) of the LUMO is calculated to be slightly larger for $Si_4S_5H_6$ than for $Si_3S_4H_4$ and the XANEs energy consequently smaller. Thus, breaking of the edge-shared chain may be observable in XANES.

Table 10. Calculated Negatives of Orbital Eigenvalues (in eV) for the HOMO and the Central Si 1s Orbital of the Neutral Molecules (Approximations to the IP) and the LUMO of the Equivalent Core Cation (Approximation to the EA) for $Si_3S_4H_4$, $Si_2S_2H_4$, and $Si_4S_5H_6$

molecule	$-\epsilon$(HOMO)	$-\epsilon$(Si 1s)	$-\epsilon$(LUMO), EICVO	XANES energy
$Si_3S_4H_4$	10.18	1863.81	3.98	1859.83
$Si_2S_4H_4$	10.19	1863.47	3.76	1859.71
$Si_4S_5H_6$	10.08	1863.76	4.47	1859.29

For Si oxides information on ∠Si–O–Si has recently been obtained from the nuclear quadrupole coupling constant of the ^{17}O nucleus using double-rotation methods.[51] Although solid-state NMR studies of quadrupolar nuclei are difficult, there is a potential for study of ∠Si–S–Si distributions and consequent determination of the type of polyhedral sharing, by measuring ^{33}S NQCC values. In Table 11 we collect electric field gradients calculated for H_2S and for some of the Si sulfide species. The dependence of the results on basis set is quite small, so that quite large molecules can be accurately treated. Our calculated EFG for H_2S is within about 2% of that recently calculated using a polarized triple-ζ basis.[52] Using the value of the nuclear quadrupole moment deduced from that study (obtained by least-squares fitting the calculated EFGs to the experimental NQCC values) we can estimate values for the NQCCs of the various sulfide species. The calculated EFGs at S are much smaller in the Si sulfides than in H_2S, as would be expected from a simple qualitative model in which the S3p orbital perpendicular to the Si–S–Si plane would be delocalized onto the Si (or Si and H) atoms. Although there is certainly some difference between the species with different ∠Si–S–Si, this difference is not so large as for the Si oxides, partly because the range of equilibrium ∠Si–S–Si angles is rather small due to the rigidity of the angle but also partly because the EFG at S seems to be much less dependent on angle. The magnitudes of the EFG components perpendicular to the

(49) Schwarz, W. H. E. *Chem. Phys.* **1975**, *11*, 217.
(50) Tossell, J. A. *Chem. Phys.* **1991**, *154*, 211.
(51) Farnan, L.; Grandinetti, P. J.; Baltisberger, J. H.; Stebbins, J. F.; Werner, U.; Eastman, M. A.; Pines, A. *Nature* **1992**, *358*, 31.
(52) Palmer, M. H. *Z. Naturforsch. A* **1992**, *47*, 203.

Table 11. Calculated Values for the Electric Field Gradient (in Atomic Units) and Estimated[a] Values of the Nuclear Quadrupole Coupling Constant e^2qQ/h (in MHz) at S in H_2S, $(H_2SiS)_n$, n = 2, 3, and $(H_2SiS)_2$, Compared with the Si–S–Si Angle

molecule	q	e^2qQ/h	∠Si–S–Si
Using the 3-21G* Optimized Geometry and the 3-21G Plus DSi3d, DS3d, H2p Basis			
H_2S	2.547[b]	38.6	94.2
$(SiH_3)_2S$			
∠=90	1.474[b]	22.3	90
equil geom			
∠=108.1	1.387[b]	21.0	108.1
∠=120	−1.492[c]	22.6	120
$(H_2SiS)_2$	1.382	20.9	83.5
Using the 3-21G* Geometry and Basis			
$(H_2SiS)_2$	1.353	20.5	83.5
$(H_2SiS)_3$ C_{3v}	1.376	20.8	103.2
$(H_2SiS)_3$ D_{3h}	1.442	21.8	119.9

[a] Assuming a nuclear quadrupole moment of −0.066 05 barn, from the Study of Palmer.[52] [b] For ∠Si—S—Si = 90 and 108.1° the largest component of q is perpendicular to the Si–S–Si plane. [c] For ∠=120° the largest component is along the Si···Si vector.

Table 12. Calculated ^{33}S NMR Shieldings (in ppm) Calculated Using 3-21G* Geometries, 3-21G + DSi3d, DS3d, H2p Basis and LORG Method for H_2S, $(SiH_3)_2S$, and $(H_2SiS)_2$

molecule	σ
H_2S	709
$(SiH_3)_2S$	
∠=90	934
∠=108.1	922.5
∠=120	923
$(H_2SiS)_2$	819
$(H_2SiS)_3$	874

Si–S–S plane and along the Si···Si vector also cross over in magnitude as the ∠Si–S–Si changes, so a significant change in the EFG tensor is not seen in the scalar NQCC. Nonetheless, it may be possible to extract some angular information from experimental ^{33}S NMR studies of the NQCC.

In Table 12 we show calculated ^{33}S NMR shieldings of H_2S and some of Si sulfides. Our calculated shielding values for H_2S is within 8 ppm of that obtained from very large basis conventional CHF calculations[53] and in reasonable agreement with the absolute shielding value estimated[54] to be 752 ppm. We find that the bridging S in $(SiH_3)_2S$ is more highly shielded than that in H_2S by more than 200 ppm and the shielding increases as the bridging angle decreases. The corresponding ^{17}O NMR shieldings of $(SiH_3)_2O$ and gaseous H_2O, on the other hand, differ by only around 10 ppm and the shielding decreases as the bridging angle decreases.[8] Compared to $(SiH_3)_2S$, the 2-ring $(H_2SiS)_2$ is calculated to be deshielded by about 100 ppm and the 3-ring $(H_2SiS)_3$ by about 50 ppm. The strong deshielding of the 2-ring may provide an additional characteristic useful for the identification of edge-sharing geometries in the Si sulfides.

Conclusions

It is clear from our results that the structural properties of corner-sharing and edge-sharing Si sulfide molecules can be accurately calculated at the polarized split-valence SCF level. Edge-sharing geometries are much more favorable for sulfides than for the analogous oxides, and completion of the Si coordination sphere by –SH groups, rather than by H or alkyl groups, further favors edge-sharing. A model with two shared edges, $Si_3S_4H_4$, yields calculated vibrational energies in good agreement with experimental results for solid SiS_2. Although most of the spectral features are assigned in the same way as in previous experimental studies, we agree with Griffiths et al. in assigning the so-called a_1^B "companion" line to a b symmetry vibration rather than a totally symmetric a. Breaking one shared edge or replacing it with a corner-sharing 3-ring increases the energy of this "companion" vibration as well as slightly shifting the energy of the main a_1 symmetry Si–S symmetric stretching mode.

Calculations on Si oxide edge- and corner-sharing molecules using the LORG method give results consistent both with experiment and with previous comon-origin CHF calculations. The Si shielding is calculated to decrease as the ∠Si–O–Si decreases and the 2-ring edge-shared molecule is calculated to be deshielded compared to the corner-shared 3-ring and higher order rings. We correctly reproduce trends in shielding for Si sulfides using the LORG method for those molecules which are small enough to be treated at the doubly polarized split valence level. For example, shieldings calculated along the series $SiH_{4-n}(SH)_n$ agree well with experimental values for the series $SiH_{4-n}(SCF_3)_n$, and the orthothiosilicate model $Si(SH)_4$ is correctly calculated to be deshielded with respect to isoelectronic $SiCl_4$. Relative shieldings of $SiH_3(SCH_3)$ and $(SiH_3)_2S$ are in reasonable agreement with experiment and the S shielding is calculated to decrease as the bridging angle decreases, just as in oxides. For the $(H_2SiS)_n$ rings, n = 2 and 3, doubly polarized basis sets could be used only for the common-origin CHF calculations and for the GIAO calculations. At this basis set level, the 2-ring is slightly shielded compared to the 3-ring, consistent with experiment.

Although it is clear that larger, more flexible basis sets will be needed to accurately calculate Si NMR shieldings in the sulfides, it also appears that the shielding of the edge-shared species is larger in the solid, where the Si is entirely coordinated by S, than it is in $(R_2SiS)_n$ gas-phase molecules. We can speculate that this difference is related to the change in energetics of the 2- and 3-rings when –SH is substituted for –H. In general, we would expect that as the hardness of the species (e.g., as measured by the HOMO–LUMO gap) increases, the paramagnetic contributions of the NMR shieldings of its atoms will tend to decrease in magnitude so that total shieldings will increase. Since increased hardness is associated with increased stability, we would expect the most stable species to have the largest shieldings. Thus, in Si oxides corner-sharing polymers have the highest stability and the largest Si NMR shieldings while in Si sulfides the edge-sharing polymers have the highest stability and largest NMR shieldings.

It is also clear that although ^{33}S is a difficult NMR nuclide, study of the NMR shielding constant may give some information on the nature of the polymerization. By contrast, the NQCC at S does not seem to be simply related to briding angle or mode of polymerization.

Acknowledgment. This work was supported by the National Science Foundation, Grant DMR 9120100. I thank G. Saghi-Szabo for assistance with the GIAO calculations.

(53) Lazzeretti, P.; Zanasi, R. *J. Chem. Phys.* **1980**, *72*, 6768.
(54) Wasylishen, R. E.; Connor, C.; Friedrich, J. O. *Can. J. Chem.* **1984**, *62*, 981.